International Journal on Magnetic Particle Imaging
Vol 12, No 1, Suppl 1, Article ID 2603047, 3 Pages

Infinite Science Publishing

Proceedings Article

Large core & small shell particles facilitate physiological viscosity differentiation via MPS

S. Bolte[a,*] · B. Simsek[a] · M. B. Abbas[a] · H.-J. Krause[b] · U. M. Engelmann[a,*]

[a] Department of Medical Engineering and Applied Mathematics, FH Aachen UAS, Jülich, Germany
[b] Institute of Biological Information Processing, Forschungszentrum Jülich, Jülich, Germany
[*] Corresponding author, email: {sandra.bolte, engelmann}@fh-aachen.de

Abstract

Magnetic nanoparticles (MNP) are researched for in-vivo applications and represent a key tool in both therapy via magnetic fluid hyperthermia (MFH) and diagnostics using magnetic particle spectroscopy (MPS) and imaging (MPI). In-vivo, MNP are exposed to various physiological environments, binding to blood and cells and are thereby subjected to constantly changing conditions. In this simulative work, the performance of MNP in MPS was investigated with regard to core size, hydrodynamic size and distribution width and under different physiological viscosities of water, blood and inside cells. Our preliminary results from stochastic Neel-Brownian coupled relaxation dynamics simulations suggest that for MPS, differentiation of MNP binding states across water, blood, and intracellular environments appears feasible for MNP of large cores above 20 nm with small hydrodynamic sizes below 50 nm.

I. Introduction

Magnetic nanoparticles (MNP) promise innovative biomedical applications in therapy - employed as heating agents in magnetic fluid hyperthermia (MFH) - and diagnostics - used as biomarkers and imaging tracers in magnetic particle spectroscopy (MPS) and imaging (MPI). All of these applications inevitably rely on MNP being administered into the body, where they interact with physiological entities such as blood and cells. Such interaction decreases the MNP's mobility over time upon adsorption of blood constituents or internalization inside cells, which is known to decrease performance for MFH [1] and MPS [2]. However, when compared to a reference of freely dispersed MNP in water, detecting such a decrease in signal could also serve as an indicator to determine the current binding state of MNP, allowing conclusions on the microenvironment that MNP are subjected to. This could eventually advance and complement MNP localization capabilities of MPS or MPI. To explore this application further, we employ stochastic simulations of MNP relaxation dynamics [3], with various core and hydrodynamic sizes to model different MNP systems and varying viscosity values to model physiologically relevant binding states of MNP in water, blood, and inside cells.

II. Methods and materials

Stochastic Neel-Brownian coupled relaxation dynamics simulations were used to model the magnetization curve, M(H), of an ensemble of 1000 particles magnetite MNP (saturation magnetization $M_S = 476 kAm^{-1}$, uniaxial anisotropy constant $K_u = 11 kJ \cdot m^{-3}$) using python framework (s. Author's statement) [3]. Using a concentration of $10^{15} mL^{-1}$ and a temperature of $T = 300$ K magnetic interactions are negligible versus thermal activation [4]. A single-frequency magnetic field was applied in two different conditions: Firstly, the influence of core and hydrodynamic size on MPS signal was investigated using core sizes of $d_C = (12, 15, 18, 22, 24, 28)$

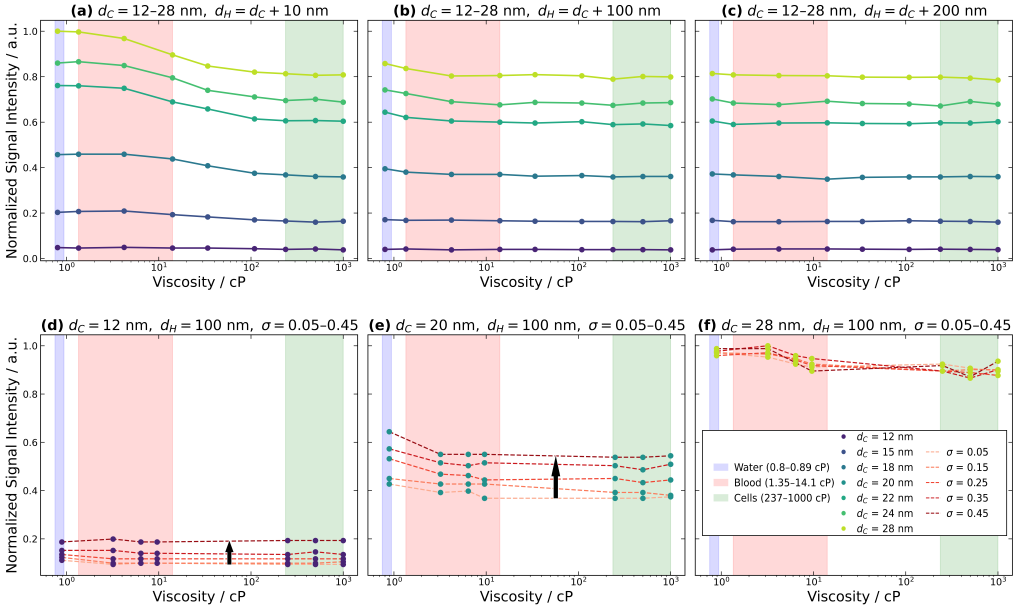

Figure 1: Simulated MPS signal intensities for various particle sizes and viscosities (s. Table 1). Subfigures ((a)-(c)) show varied core sizes $d_C = (12-28)$ nm ($\sigma = 0.05$) for three hydrodynamic diameters at applied field of $H_1 = 25$ mT/μ_0 and $f_0 = 25$ kHz. Intensities normalized to maximum ($d_C = 28$ nm, $d_H = 38$ nm, water). Subfigures ((d)-(f)) show varying size distribution widths $\sigma = (0.05-0.45)$ at applied field of $H_2 = 20$ mT/μ_0 and $f_0 = 25$ kHz. The corresponding core diamrters are (d) $d_C = 12$ nm, (e) $d_C = 20$ nm, and (f) $d_C = 28$ nm, with $d_H = 100$ nm in all cases. Intensities normalized to maximum ($d_C = 28$ nm, $\sigma = 0.35$ nm, blood).

Table 1: Physiological viscosity ranges used for simulations.

Water / Ref	0.89 cP
Blood / cytoplasm	(1.35, 3.20, 4.21, 6.40, 9.60, 14,10) cP
Interim region	(33.90, 109.00) cP
Intracellular	(237.00, 250.00, 500.00, 1000.00) cP

nm, each with monodisperse log-normal distribution width ($\sigma = 0.05$) and three hydrodynamic diameters: $d_H = d_c + (10, 100, 200)$ nm. Field conditions where $H_1 = 25$ mT/μ_0 at $f_0 = 25$ kHz. Secondly, the influence of the core size distribution was investigated for the mean core sizes $d_C = (12, 20, 28)$ nm each of distribution widths $\sigma = (0.05, 0.15, 0.25, 0.35, 0.45)$ and fixed $d_H = 100$ nm. The MNP were subjected to $H_2 = 20$ mT/μ_0 at $f_0 = 25$ kHz. In both cases, the viscosity of the surrounding medium, η, was systematically varied to represent different physiologies listed in Table 1 based on literature [5,6].

From simulated M(H)-loops the transient phase was removed prior to smoothening each curve (employing Savitzky–Golay filtering). The smoothed curves were differentiated, yielding the derivative dM/dH, from which the maximum was extracted and is given as a performance indicator for MPS signal intensity, which is directly proportional to dM/dH [7].

III. Results and discussion

Figure 1 shows the dependence of MPS signal intensity on viscosity, as well as for various core and hydrodynamic sizes ((a)-(c)) and core size distributions ((d)-(f)). Figure 1(a) through (c) confirms common expectation that MPS signal increases dominantly with MNP core size [7], with strongest signal for large d_C and small d_H, maximized with field amplitude (cf. Figure 1(a) and (d)). We furthermore observe that for small hydrodynamic sizes $d_H = d_C + 10$ nm (Figure 1(a)) the MPS signal drops from highest values in water to smaller values inside cells, with the strongest drop by $\approx -15\%$ for largest MNP with $d_C = 28$ nm, while negligible for $d_C = 12$ nm, in accordance with recent experiments [8,9]. A similar drop, but much less pronounced (max. drop by $\approx -6\%$), is observed for larger hydrodynamic sizes, $d_H = d_C + 100$ nm (Figure 1(b)), but indistinguishable for $d_H = d_C + 200$ nm (Figure 1(c)), which in fact seems independent of viscosity at all. Thus, we conclude that (for the given setting) differentiating physiologically relevant viscosities requires small hydrodynamic sizes $d_H < 50$ nm [9]. While MNP systems in Figure 1 ((a)-(c)) where monodisperse, Figure 1((d)-(f)) investigates the dependence of MNP signal for increasingly polydisperse MNP systems with distribution widths up to $\sigma = 0.45$ for selected core sizes. Again this confirms, MPS signal increase with core size [7]. However, by simply using more polydisperse MNP (i.e. up to $\sigma = 0.45$), MPS signal intensity increased

10.18416/ijmpi.2026.2603047

relative to monodisperse MNP ($\sigma = 0.05$) by up to +100% for $d_C = 12$ nm and up to +50% for $d_C = 20$ nm, independent of viscosity. At the same time MPS signal remained effectively unaffected by σ for $d_C = 28$ nm, presumably because the simulation runs invalid as MNP approach the ferromagnetic regime.

IV. Conclusion

Preliminary results show that MPS signal intensity depends on core size and its distribution, hydrodynamic size, and viscosity. Core size generally dominates the signal, while viscosity has negligible influence for particles well above $d_H \geq 100$ nm. For viscosity-based localization, differentiation of MNP binding states across water, blood, and inside cells seems feasible for large cores $d_C \geq 22$ nm and small shell $d_H < 50$ nm (Figure 1(a)). Increased polydispersity may enhance MPS signal for mid-sized MNP systems ($d_C = 20$ nm, Figure 1(e)), offering optimization potential for in-vivo MPS via MNP adaptation. However, to guide discussion further, our model must first account for magnetic interaction effects upon intracellular agglomeration of MNP.

Acknowledgments

The authors state no funding involved but gratefully acknowledge computational resources provided by FH Aachen UAS (FB9).

Author's statement

Authors state no conflict of interest.

Source code used for simulations can be accessed at https://github.com/cshasha/nano-simulate "Engelmann 2021".

References

[1] U. M. Engelmann et al. „Combining bulk temperature and nanoheating enables advanced magnetic fluid hyperthermia efficacy on pancreatic tumor cells", *Scientific Reports*, vol. 8, no. 1, pp. 13210, 2018, doi: 10.1038/s41598-018-31553-9.

[2] E. Teeman, C. Shasha, J. E. Evans and K. M. Krishnan, "Intracellular dynamics of superparamagnetic iron oxide nanoparticles for magnetic particle imaging", *Nanoscale*, vol. 11, no. 16, pp. 7771-7780, 2019, doi: 10.1039/c9nr01395d.

[3] U. M. Engelmann, C. Shasha and I. Slabu, *Magnetic Nanoparticle Relaxation in Biomedical Application*, in Magnetic Nanoparticles in Human Health and Medicine: Current Medical Applications and Alternative Therapy of Cancer, 1st ed., C. Caizer, Ed. Hoboken, John Wiley & Sons, 2021, pp. 327–354, doi: 10.1002/9781119754725.ch15.

[4] U. M. Engelmann, A. Shalaby, C. Shasha, K. M. Krishnan, and H.-J. Krause, "Comparative Modeling of Frequency Mixing Measurements of Magnetic Nanoparticles Using Micromagnetic Simulations and Langevin Theory," *Nanomaterials*, vol. 11, no. 5, 2021, doi: 10.3390/nano11051257.

[5] O. E. Puchkov et al. "Intracellular viscosity: Methods of measurement and role in metabolism." *Biochemistry (Moscow) Supplement Series A: Membrane and Cell Biology*, vol. 7 no. 4, pp. 270-279, 2013, doi: 10.1134/S1990747813050140.

[6] A.S. Kashirina et al. "Monitoring membrane viscosity in differentiating stem cells using BODIPY-based molecular rotors and FLIM" *Scientific Reports*, vol. 10, no. 1, pp. 14063, 2020, doi: 10.1038/s41598-020-70972-5.

[7] H.-J. Krause and U. M. Engelmann "Fundamentals and Applications of Dual-Frequency Magnetic Particle Spectroscopy: Review for Biomedicine and Materials Characterization", *Advanced Science*, vol. 12, no. 13, pp. 2416838, 2025, doi: 10.1002/advs.202416838.

[8] K. Rathi et al. "Assessment of differential magnetic susceptibility in nanoparticles: Effects of changes in viscosity and immobilisation", *Journal of Magnetism and Magnetic Materials*, vol. 514, no. 167238, 2020, doi: 10.1016/j.jmmm.2020.167238.

[9] A. Remmo et al. " Immobilization-induced anomalous dynamic magnetization effect in synomag nanoparticles as tracers for magnetic particle imaging", *ACS Applied Nano Materials*, vol. 7, no. 21, pp. 24315–24324, 2024, doi: 10.1021/acsanm.4c01523.

